A Potent Inhibitor of Aminopeptidase P2 Reduces Reperfusion Injury in Models of Myocardial Infarction and Stroke[S]

Morgan R. Lenz, Shih-Yen Tsai, Anne E. Roessler, Yang Wang, Periannan Sethupathi, W. Keith Jones, Gwendolyn L. Kartje, and William H. Simmons

Department of Molecular Pharmacology and Neuroscience, Stritch School of Medicine Health Sciences Division, Loyola University Chicago, Maywood, Illinois (M.R.L., A.E.R., Y.W., P.S., W.K.J., G.L.K., W.H.S.) and Research Service, Edwards Hines Jr. VA Hospital, Hines, Illinois (S.-Y.T., G.L.K.)

ABSTRACT

During a myocardial infarction or ischemic stroke, blood flow to the heart or brain is partially blocked. This results in reduced delivery of oxygen and nutrients and, ultimately, tissue damage. Initial treatment involves removing the clot and restoring blood flow (reperfusion). However, this treatment is not as effective as one would hope because the reperfusion process itself can cause a different type of damage (reperfusion injury) that contributes up to 50% of the total damage. Bradykinin is an autocoid that is released from blood vessel endothelial cells during ischemia and reperfusion and has the potential to prevent reperfusion injury. However, bradykinin is rapidly inactivated by enzymes on endothelial cells, limiting its beneficial effects. One of these enzymes is aminopeptidase P2. We designed a potent and specific inhibitor of aminopeptidase P2 called ST-115, [(S)-2-mercapto-4-methylpentanoyl]-4(S)-fluoro-Pro-Pro-3(R)-beta-Pro. When ST-115 is administered intravenously at the start of reperfusion, it reduces bradykinin degradation. This increases bradykinin's concentration in the capillaries and enhances its protective effects. We tested ST-115 in a mouse model of myocardial infarction and found that the damaged area of the heart was reduced by 58% compared with mice given saline. In a rat model of ischemic stroke, ST-115 reduced functional deficits in a skilled walking test by 60% and reduced brain edema by 51%. It reduced brain infarct size by 48% in a major subset of rats with small strokes. The results indicate that ST-115 can ameliorate reperfusion injury and can ultimately serve as a therapeutic for acute myocardial infarction and ischemic stroke.

SIGNIFICANCE STATEMENT

We have shown that our aminopeptidase P2 inhibitor, ST-115, can reduce tissue injury caused by episodes of ischemia followed by reperfusion. It was successful in rodent models of myocardial infarction and stroke. The clinical use would involve the intravenous administration of ST-115 at the induction of reperfusion. In the case of stroke, the successful technique of thrombectomy could be combined with ST-115 administration to simultaneously reduce both ischemic and reperfusion injury.

Introduction

Acute myocardial infarction and ischemic strokes are among the leading causes of death and disability in westernized societies. They occur because of clots that block arteries and reduce the amount of blood flowing through the tissue. The result is ischemia, which leads to tissue damage. Current treatments are limited to dissolving the clot with the enzyme, tissue plasminogen activator, and/or by mechanically pulling the clot out of the artery (thrombectomy). The result is restoration of blood flow, called "reperfusion." Although reperfusion is the main goal of these treatments, it is not as effective as one would hope. This is because the reperfusion process itself causes a different type of tissue damage called "reperfusion injury", which can be initiated within minutes of the start of reperfusion. This injury involves a complicated set of biochemical changes that leads to one of several types of cell death (Kalogeris et al., 2016). Reperfusion injury accounts for at least 50% of the total tissue damage that occurs during ischemia/reperfusion (Hausenloy and Yellon, 2013).

Preclinical and clinical studies have indicated that a potential therapeutic is the endogenous peptide bradykinin. Bradykinin mediates the protective effects of cardiac pre- and postconditioning techniques (Murry et al., 1986; Zhao et al., 2003; Critz et al., 2005) as well as protection by angiotensin converting enzyme inhibitors (Hartman, 1995; Wolfrum et al., 2001; Erşahin et al., 1999). During ischemia and reperfusion, bradykinin is released from the endothelial cells that line the wall of blood vessels. It has the potential to activate tissue survival pathways (Bellis et al., 2020). However, without a conditioning stimulus, bradykinin concentrations are not high enough to protect. Administering bradykinin itself to increase concentrations would not be safe, as this could cause a serious

ABBREVIATIONS: ACE, angiotensin converting enzyme; B$_2$, bradykinin B$_2$ receptor; CCA, common carotid arteries; CI, confidence interval;, ; K_i, the dissociation equilibrium constant of an enzyme-inhibitor complex; K_m, Michaelis constant (the concentration of the substrate at which the enzyme is at half maximal velocity); MCA, middle cerebral artery; ST-115, [(S)-2-mercapto-4-methylpentanoyl]-4(S)-fluoro-Pro-Pro-3(R)-beta-Pro; TTC, triphenyltetrazolium chloride.

drop in blood pressure if the dose were too high. Therefore, we chose to modestly increase endogenous bradykinin by partially blocking its metabolism. In our previous studies, we perfused radiolabeled bradykinin through the pulmonary and coronary vasculatures of rats with and without specific enzyme inhibitors to determine how endothelial cells cleave and inactivate bradykinin. We collected the effluent from the tissues and used high-performance liquid chromatography to separate, identify, and quantify the labeled products of the enzymatic degradation of bradykinin. We found that the enzymes aminopeptidase P2 (also called X-prolyl aminopeptidase 2) and angiotensin converting enzyme (ACE) are responsible for 30% and 70%, respectively, of the inactivation of bradykinin in blood vessels (Prechel et al., 1995; Erşahin and Simmons, 1997). Both enzymes are located on the inside wall (luminal membrane) of vascular endothelial cells where bradykinin is produced. We purified aminopeptidase P2 and showed that it could inactivate bradykinin by breaking the peptide bond between Arg and Pro and releasing the first Arg (Simmons and Orawski, 1992; Orawski and Simmons, 1995; Simmons, 2015): Arg-Pro-Pro-Gly-Phe-Ser-Pro-Phe-Arg.

We developed the first inhibitor of aminopeptidase P2, called apstatin (Prechel et al., 1995). We used apstatin in an isolated perfused rat heart model of ischemia/reperfusion and showed that it significantly reduced ischemia/reperfusion injury (Erşahin et al., 1999). Other laboratories then studied rats with an acute myocardial infarction and found about a 50% protection by apstatin (Wolfrum, et al., 2001; Veeravalli et al., 2003). In all cases, the protective effect of apstatin was blocked by the bradykinin B_2 receptor antagonist icatibant (HOE140). This indicated that the protective effect is due to an increase in endogenous bradykinin signaling. Inhibitors of nitric oxide synthase and cyclooxygenase each partially inhibited the protection, suggesting that nitric oxide and prostacyclin may be secondary mediators of bradykinin (Veeravalli et al., 2003). We have since developed a much more potent and specific aminopeptidase P2 inhibitor, [(S)-2-mercapto-4-methylpentanoyl]-4(S)-fluoro-Pro-Pro-3(R)-beta-Pro (ST-115) (Fig. 1) (Simmons, 2015). It has been shown to reduce reperfusion injury in an acute kidney injury model (Simmons, 2015). Based on the above data, a putative mechanism about how this compound can reduce reperfusion injury is shown in Fig. 2. During ischemia and reperfusion, capillary endothelial cells release bradykinin. Aminopeptidase P2, which is on the membrane of endothelial cells, participates in the cleavage and inactivation of bradykinin, such that little of it reaches B_2 receptors. When ST-115 is administered intravenously at the start of reperfusion (Fig. 2), it binds to the active site of aminopeptidase P2 and blocks the enzyme's ability to cleave bradykinin. As a result, there is an increase in the concentration of intact bradykinin, which then binds to B_2 receptors on the endothelial cells. Bradykinin stimulates these cells to synthesize and release compounds known to
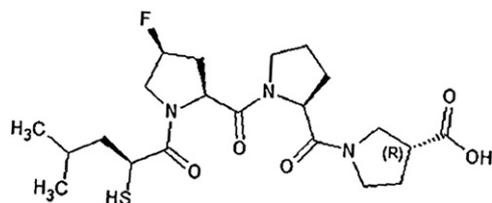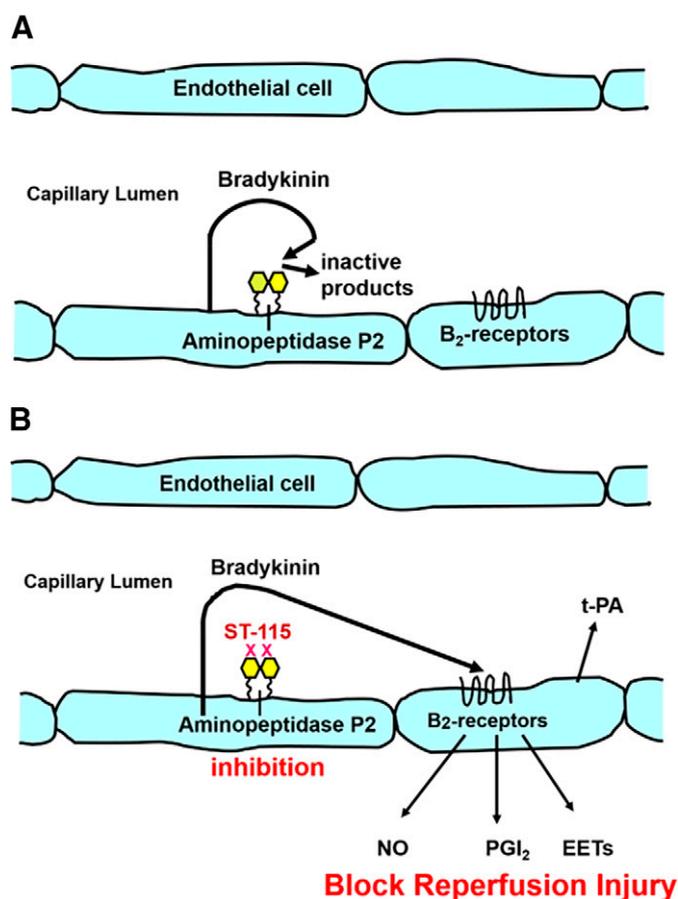
Fig. 2. The proposed mechanism for reducing reperfusion injury by administering an inhibitor of aminopeptidase P2 and increasing bradykinin. (A) No inhibitor present: Bradykinin is released into blood capillaries from vascular endothelial cells during ischemia and reperfusion. With no inhibitor present, aminopeptidase P2 (yellow) cleaves bradykinin into an inactive fragment. There is not a sufficient amount of active bradykinin to bind to and activate bradykinin B_2 receptors. (B) When an inhibitor of the enzyme is present (ST-115 or apstatin), it binds to the active site of aminopeptidase P2 and prevents bradykinin from binding to the enzyme and being cleaved. As a result, the concentration of active bradykinin increases. The bradykinin then binds to the B_2 receptors on endothelial cells and stimulates the release of nitric oxide, prostacyclin (PGI_2), and epoxyeicosatrienoic acids (EETs) (all of which are known to reduce reperfusion injury), and tissue plasminogen activator, which can initiate clot dissolution. (Not shown are angiotensin converting enzyme and its inhibitors, which can function in parallel with aminopeptidase P2 and its inhibitors in this mechanism.)

reduce reperfusion injury. They include nitric oxide (Critz et al., 2005), prostacyclin (Penna et al., 2008), and epoxyeicosatrienoic acids (EETs) (Gross et al., 2005; Weston et al., 2005; Tu et al., 2018). Bradykinin also releases the enzyme tissue plasminogen activator to prevent clot formation (Brown et al., 2000). This is a rare situation where one drug can produce multiple protection mediators.

This current report describes the chemical properties of ST-115 and provides data that test two hypotheses: that ST-115 can reduce reperfusion injury in 1) a mouse model of myocardial infarction and 2) a rat model of ischemic stroke. t-PA= tissue plasminogen activator, NO=nitric oxide

Materials and Methods

Ethical Approvals. Mice were maintained, and experiments were approved by the Loyola Institutional Animal Care and Use Committee,

Fig. 1. The structure of ST-115.

following the institutional guidelines, and the Guide for the Care and Use of Laboratory Animals (NIH, Eighth edition, The National Academies Press, Washington, D.C., 2011). The Loyola facilities are Association for Assessment and Accreditation of Laboratory Animal Care accredited and compliant.

The stroke experiments involving rats were approved by the institutional animal care and use committee at Edward Hines Jr. Veterans Affairs Hospital, permit Hi8-006, and carried out in Association for Assessment and Accreditation of Laboratory Animal Care-accredited facilities in full compliance with the standards for the care and use of laboratory animals.

ST-115. ST-115 contains a thiol group (Fig. 1) that is susceptible to oxidation by dissolved oxygen in solution to form disulfide-linked homodimers. This thiol group presumably binds to a zinc ion in the enzyme active site and is essential for inhibiting the enzyme. The homodimer is inactive. Stock solutions of ST-115 were prepared in water, aliquoted, and stored at $-20°C$. A 5-mM solution of ST-115 in water has a pH of 2.95 due to the presence of the carboxylic acid group. This low pH suppresses disulfide formation in solution (Torchinskii, 1974). Nevertheless, stock solutions of ST-115 were frequently tested for the concentration of free thiol groups by a chemical assay based on 5,5′-dithio-bis-(2-nitrobenzoic acid) (DTNB) (Ellman's Reagent) (Sigma-Aldrich, St. Louis, MO). An example of the assay is as follows: To a 1.5 ml, 1 cm path methacrylate cuvette was added 1) 0.95 ml of 0.1 M Hepes, pH 7.4, buffer; 2) 0.05 ml of 10 mM DTNB in the same buffer; and 3) 5 µl of 5 mM ST-115. After 10 minutes, the absorbance of the yellow samples was quantified by reading the cuvettes in a Beckman Coulter DU 7400 spectrophotometer at a wavelength of 412 nm. The mean absorbance of controls (without ST-115) was subtracted from the mean absorbance of the ST-115 samples. The difference between absorbances was then used to calculate the concentration of the thiol groups via the following equation: (ΔAbs $\div$ 14,150 M^{-1}) $\times$ (200) $\times$ (I000 mM/M) = [–SH] (in mM), where 200 is the dilution factor for the 5 µl of ST-115 in the assay and 14,150 M^{-1} is the molar absorption coefficient per centimeter for the yellow reaction product, 2-nitro-3-thiobenzoate anion (Riddles et al., 1983).

The concentration of ST-115 in freshly prepared solutions as determined by the DTNB assay was consistently lower by about 14% than the calculated concentration based on weight. This suggests the presence of non-thiol content in the ST-115 powder, presumably water, which is frequently present in lyophilized peptides. The calculation of the weight of ST-115 that is required to make a solution of a specific concentration is improved by including the multiplication factor of 1.14.

Preparation of Sample Tubes Containing Dried ST-115 for Storage, Transport, and Injection. The doses of ST-115 that were administered to animals to reduce reperfusion injury were 10 µg/kg for mice (myocardial infarction study) and 16 µg/kg for rats (stroke study). These quantities were too small to weigh out individually. Furthermore, very dilute stock solutions are susceptible to oxidation of the thiol group of ST-115 at neutral pH and room temperature. Therefore, individual microfuge tubes containing dried ST-115 were prepared ahead of time. The following is an example of the preparation of a tube for a rat: A 5.0-mM stock solution of ST-115 in water was used, as the intrinsic low pH (2.95) would prevent thiol oxidation during preparation. An aliquot (3.5 µl) of this solution was transferred to a 1.5-ml polypropylene microfuge tube. The tube was loosely covered with foil to allow for evaporation of the water overnight. The dried ST-115 (8 µg) was chemically stable and remained completely in the free thiol form for at least 4 months at room temperature. This was shown by carrying out the DTNB reaction within the tubes at different time points. Therefore, the dried samples could be stored or transported without fear of chemical modification. Furthermore, the amount of dried ST-115 was so small that it was not visible in the bottom of the tube, which maintained blinding. For an in vivo ischemia/reperfusion experiment, 1 ml of sterile physiologic saline (0.9% w/v NaCl) was added to the tube just prior to reperfusion. After mild vortexing, a volume of the ST-115 solution equivalent in ml to 2 × kg of body weight was injected into the tail vein (rat) or jugular vein (in mice). The

following is an example for a 300-g rat using three different but equivalent calculations: (2 × 0.3 kg = 0.6 ml) *or* (dose × 1/concentration × weight) *or* (16 µg/kg × ml/8 µg × 0.3 kg).

After the injection, the remainder of the solution was discarded, as oxidation can slowly occur in the dilute solution. A separate tube was used for each animal.

In Vitro Studies

The IC_{50} Value (an Indication of Binding Affinity) for ST-115 Inhibition of Aminopeptidase P2. Human aminopeptidase P2 enzyme was highly purified from human kidney tissue using the scheme described previously (Simmons, 2015). Enzyme activity was determined by a fluorescence assay that uses the internally quenched substrate H-Lys(2-aminobenzoyl)-Pro-Pro-p-nitroanilide (Bachem, Torrance, CA) (Stöckel-Maschek et al., 2003). The reaction was carried out at 30°C in black polypropylene microplate wells (Greiner Bio-One, Monroe, NC) containing 0.1 M Hepes, pH 7.4, and a substrate concentration of 1 µM, which is equivalent to the Michaelis constant (K_m). Cleavage of the substrate in front of the first Pro by the enzyme increases the fluorescence by removing the p-nitroanilide quencher. The rate of substrate cleavage over 35 minutes (expressed as an increase in fluorescence units per minute) was measured in an f-Max fluorescence filter microplate reader (Molecular Devices, Sunnyvale, CA) set in kinetics mode. The excitation wavelength was 320 nm, and the emission wavelength was 405 nm. Controls without enzyme were included in each run, and the fluorescence drift rate was subtracted from the enzyme rates. Fifteen different concentrations of ST-115 were tested over the range of 10^{-12} to 10^{-5} M and plotted on a semilogarithmic scale. Each data point was the average of four technical replicates. The data were analyzed using the Prism 8.3 program (GraphPad, San Diego, CA) that was set up for 1) nonlinear regression, 2) dose–response curves inhibition, 3) log inhibitor versus response, and 4) variable slope. The binding affinity of ST-115 for aminopeptidase P2 was expressed as an IC_{50} value (the concentration that inhibits enzyme activity by 50% compared to control activity without inhibitor.

The Specificity of ST-115. ST-115 was tested for its ability to inhibit 20 different peptidases and proteolytic enzymes. These included other enzymes that have the ability to cleave peptides next to proline residues and/or to use metal ions to carry out hydrolysis of a peptide bond. A detailed description of each enzyme, its source, its substrate, and the assay conditions are included in the Supplemental Material. In general, each enzyme was initially assayed at different substrate concentrations to determine an approximate K_m value. A substrate concentration that was either at or below the K_m was chosen for determining ST-115 inhibition. Initial rates were determined. This setup gave IC_{50} values in a narrow range between the dissociation equilibrium constant of an enzyme-inhibitor complex (K_i) and $2K_i$ assuming competitive inhibition, allowing semiquantitative comparison among enzymes (Cheng and Prusoff, 1973). IC_{50} values could not be determined for several of the weakly inhibited enzymes because of limited amounts of enzyme and/or reagents. In these cases, the results are shown as "greater than" ($>$) the highest concentration of ST-115 tested.

In Vivo Studies

Mouse Model of Myocardial Infarction.

Experimental design. The hypothesis is that ST-115 reduces infarct size in mice subjected to a period of cardiac ischemia–reperfusion when it is administered intravenously just before the start of reperfusion. The study was carried out in a fully blinded manner at all steps with respect to whether each mouse was administered saline vehicle or ST-115.

Surgery. Mice were male B6129SF2/J (Jackson Laboratory, stock 101045) 11–12 weeks of age, and ranged from 28.7 g to 36.9 g at the time of surgery. They were housed individually before and after surgery to prevent fighting. Mice were anesthetized by intraperitoneal injection of sodium pentobarbitol (90 mg/kg), and a lateral thoracotomy was performed between the second and third ribs. An 8-0 nylon suture was

used to make a reversible ligature around the left anterior descending coronary artery 2–4 mm from the tip of the left auricle. Tightening the ligature caused ischemia, which was reversed after 45 minutes. ST-115 (10 μg/kg) or saline (0.9%) was administered via the jugular vein after 40 minutes of ischemia and 5 minutes before reperfusion (see above for the calculation of volumes) (Ren et al., 2004; Luther et al., 2018). Successful ischemia and reperfusion was assessed by reversible ST-segment elevation during continuous monitoring. Body temperature was maintained between 33.5°C and 36.5°C using a rectal probe thermometer and a feedback-regulated heating pad throughout the experiment and recovery. Mice recovered and were then euthanized 24 hours later by sodium pentobarbitol overdose.

After ischemia/reperfusion, the suture around the left anterior descending coronary artery remained in place, was tightened, and the heart perfused with phthalo blue (Heucotech, #515303) to stain the region blue that was not at risk. The suture was then opened, and the heart perfused through the aorta with 1% triphenyltetrazolium chloride (TTC) in PBS (pH 7.4), at 37°C using 60 mm Hg (∼3 ml over 3 minutes) of pressure, which stained viable tissue brick red. The heart was then removed and placed at −20°C until partly frozen and sectioned into 4–5 1-mm-thick transverse sections. Sections were weighed and photographed and these data used to quantify 1) area not at risk, 2) area at risk (red and infarct area), and 3) infarct size (white only) using National Institutes of Health Image J. Infarct size was expressed as the percent of infarct over area at risk, as previously described (Fishbein et al., 1981).

The number of mice used in this study was determined from preliminary studies and power analysis (seven for saline and six for ST-115 treatment). Exclusion criteria were 1) the body temperature dropped below 33°C or rose above 37.0°C (none in this study), 2) there was not ECG evidence of successful ischemia and timely reperfusion (none in this study), or 3) if mice died before reperfusion reached 24 hours' recovery (two; one died early in recovery and one overnight). When the data were unblinded, it was observed that the two mice that did not survive full reperfusion were in the saline group. Therefore, infarct size data were available for five saline and six ST-115 mice.

Rat Model of Ischemic-Reperfusion Stroke.

Experimental Design. The hypothesis is that ST-115 reduces neurologic damage in rats subjected to a period of ischemia–reperfusion stroke when it is administered intravenously just before the start of reperfusion. The study was carried out in an exploratory manner, which included open-label drug/control and post hoc statistical analysis. The parameters were measured functional deficits in the skilled horizontal ladder rung walking test, brain edema, and infarct size. The timeline for the procedures is shown in Fig. 3. All animals underwent 90 minutes of extraluminal transient middle cerebral artery occlusion along with bilateral common carotid artery occlusion to reduce spontaneous reperfusion through the collateral circulation. The
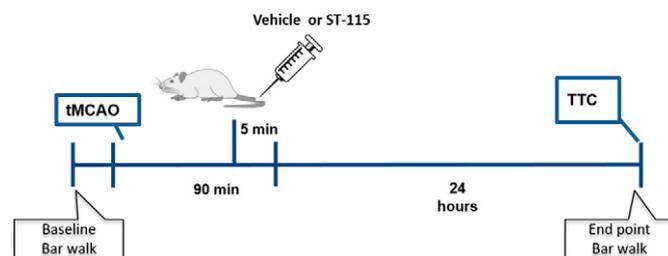
Fig. 3. Timeline for the transient middle cerebral artery occlusion stroke study. Rats first underwent three baseline trials in the skilled horizontal ladder rung walking test ("bar walk"). This was followed with a 90-minute transient middle cerebral artery occlusion (tMCAO). Five minutes before the start of reperfusion, rats were injected with ST-115 or saline through the tail vein. Reperfusion was initiated and then carried out for 24 hours. Rats then underwent three post-reperfusion trials of the bar walk test followed by decapitation. Brain sections were analyzed for infarct size after treatment with TTC.

extraluminal stroke model was used instead of an intraluminal filament model because it has a decreased risk of vessel damage and allows direct observation of blood flow through the middle cerebral artery (MCA). It also produces a stroke that is more commonly seen in human patients, such as cortical damage without striatal damage (Sommer, 2017).

Twenty-eight 10-week-old male Sprague-Dawley rats (300–350g) (Envigo,IN) were used in these studies. Rats were housed in pairs in a nonsterile microisolator cage with a filter top and kept on a 12-hour light/dark cycle with food and water available ad libitum. All surgeries and behavior tests were conducted between 10 AM and 5 PM, Monday through Friday.

Surgery. Rats were placed in a plexiglass box and anesthetized using 75 mg/ml of isoflurane delivered as an inhalant (5% isoflurane in 100% oxygen). For the remainder of the surgery, rats were kept anesthetized with 2–3% isoflurane in oxygen through a nose mask. Core body temperature was maintained between 37°C and 38°C during the procedure via a warming plate with feedback temperature control (TCAT-2DF, Harvard Apparatus, Holliston, MA). At the beginning of the procedure, a midline longitudinal cervical neck incision was made, and the bilateral common carotid arteries (CCA) were isolated. Rats were then placed in a stereotaxic frame, and a 2-cm vertical incision was made between the left eye and ear. The temporalis muscle was then retracted, and a burr hole was made over the left parietal cortex to expose the left MCA. An additional burr hole (1.5 mm in diameter) was drilled at 1 mm posterior to bregma and 4 mm lateral to bregma on the MCAO side. A laser Doppler probe was placed on top of this burr hole and connected to a laser Doppler flowmetry system (PerFlux 5000) to monitor the blood flow after occlusion and reperfusion.

For occlusion, the MCA was followed to where it transverses the rhinal sulcus, where it was lifted with a MV-135 needle such that blood flow was visibly occluded. Immediately following the onset of occlusion, both CCA were transiently occluded with microaneurysm clips. After 85 minutes of occlusion (or 5 minutes prior to releasing the vessels), ST-115 (16 μg/kg) was injected intravenously through the tail vein (see the example calculation described above). Control rats were subjected to identical surgical procedures but were injected with the same volume of saline alone. Five minutes after the intravenous injection of ST-115 or saline, the MV-135 needle and CCA clips were removed to allow for reperfusion, and the incisions were closed. Each rat was kept warm in a separate cage and monitored during the postop period until fully awake, when it was placed back into its home cage. Rats were excluded from this study if there were significant problems with MCA occlusion (e.g., rupture, too deep for occlusion) or if they died in surgery. Three rats were excluded from the study for these reasons.

The dose of ST-115 used in this experiment was based on preliminary studies in rats exposed to 45-minute ischemia and treated with 5–50 μg/kg ST-115 at reperfusion. Although the infarct size data tended to exhibit a lognormal distribution (see discussion below), the 16-μg/kg dose was the lowest dose that gave a repeatable reduction in infarct volume.

The Skilled Horizontal Ladder Rung Walking Test. The skilled horizontal ladder rung walking test was used to assess forelimb and hindlimb placing, stepping, and interlimb coordination in rats with a cortical lesion. The dimensions of our ladder mirrored those originally developed by Metz and Whishaw (Metz and Whishaw, 2002). The horizontal ladder was 1 m in length and 10 cm in width, with randomly spaced, thin metal rungs measuring 1 cm to 5 cm apart and surrounded with a clear plexiglass wall on either side. The ladder was placed 30 cm above the ground, with the rat's home cage at the end of the ladder. For each trial, animals were guided to walk from one end to the other in one direction, and each animal was guided in the same direction to keep consistency between animals and rung pattern. All trials were video recorded for later analyses. Videos were assessed for the number of total steps and the number of slips taken by the right (impaired) forelimb during each trial. A slip was defined

as when the limb either slipped off the rung or missed the rung, both of which resulted in a disruption of weight placement. All rats underwent three trials prior to transient middle cerebral artery occlusion for baseline measurement. Animals were tested again in three additional trials at 24 hours post reperfusion. The number of total steps and slips were recorded for each trial, and the data were converted to the number of slips per 10 steps taken. The value for the baseline was subtracted from the post-stroke value to remove the intrinsic capability of the rat and therefore isolate the effect of the stroke and stroke + ST-115 on the walking deficits.

Measurement of Brain Edema. Brain edema was calculated from the TTC-stained sections (see below) according to (Kuts et al., 2019): The Extent of brain edema = (Σ intact ipsilateral hemisphere − Σ contralateral hemisphere area) ÷ (Σ contralateral hemisphere area) × 100. For statistical analysis, "brain edema" data points were labeled as "percent increase" over the unaffected contralateral hemisphere area.

Sections were not used for analyzing edema if the ipsilateral hemisphere volume was measured to be less than that of the contralateral hemisphere, potentially indicating uneven sectioning. Four rats were excluded from the study for these reasons. Overall, data for brain edema were obtained from 18 rats ($N = 8$ for vehicle, and $N = 10$ for ST-115).

Measurement of Infarct Volume. After 24 hours of reperfusion, which included the skilled walking test, rats were first anesthetized with 5% isoflurane in oxygen through inhalation. Once anesthetized, animals received a Euthasol solution overdose (390 mg/kg) via intraperitoneal injection. Decapitation proceeded once animals ceased respiration and were unresponsive. Brains were rapidly removed and stained with 2,3,5-triphenyltetrazolium chloride (TTC) (Sigma Aldrich, St. Louis, MO) to assess infarct volume. TTC stains the metabolically active tissues red, whereas metabolically inactive tissues are white. Two-millimeter-thick sections were stained in a 2% TTC solution in saline in the dark for 15 minutes at room temperature. Sections were then transferred to 4% paraformaldehyde (Sigma Aldrich) and stored at 4°C. For analysis, TTC sections (excluding olfactory bulb and cerebellum) were placed on a slide and scanned to a desktop computer using a Canon CanoScan LiDE 700F scanner. The contralateral, intact ipsilateral, and infarct areas were measured using Adobe C55 (47 pixels/mm). Corrected infarct areas (corrected for edema) and infarct volume were calculated as follows (Kuts et al., 2019): corrected infarct area = infarct area × contralateral hemisphere area ÷ intact ipsilateral hemisphere area. Infarct Volume = Σ corrected infarct area ÷ Σ contralateral hemisphere area × 100. For statistical analysis, "infarct volume" was expressed as a "percentage of the unaffected contralateral hemisphere".

Sections from some brains did not stay together and were not available to be analyzed for lesion volume or edema. This occurred for two animals in the study. Overall, infarct volume data were obtained from 23 rats ($N = 11$ for vehicle, and $N = 12$ for ST-115.)

Statistics for In Vivo Experiments

The statistical analysis of the mouse myocardial infarct study was carried out using the Prism 8.3 unpaired t test, as it was part of the plan for that experiment. However, post hoc statistical analysis of these data as well as the data from the rat ischemia–reperfusion stroke experiments focused on effect sizes and 95% confidence intervals (CI), as strongly encouraged by the new author guidelines for this journal (Michel et al., 2020). Estimation statistics were applied via a free web application (http://www.estimationstats.com) (Gardner and Altman, 1986; Ho et al., 2019). Control and ST-115 data were entered as two independent groups. The difference between the group means (the effect size) as well as the 95% CI (precision) were determined by bootstrapping. This involves resampling and replacement from observations 5000 times. The results were presented as a Gardner-Altman type plot (Gardner and Altman, 1986; Ho et al., 2019). A guide for interpreting these plots is included in the Fig. 5 legend.

In recognition of the fact that null-hypothesis significance testing is still being used in biology, this program also calculates the P value of the two-sided permutation t test. This value is included in the text along with the effect size and the 95% CI. The term, "not statistically significant", was used only to refer to an outcome where $P > 0.05$.

To predict the clinical significance of ST-115 treatment if human trials would have outcomes similar to those in the rat studies, the effect sizes were converted to percent "relative risk reduction" values according to the following equation: difference between the means ÷ vehicle mean × 100.

Results

In Vitro Studies

Properties of ST-115. The structure of ST-115 is shown in Fig. 1. Chemically, it is [(S)-2-mercapto-4-methylpentanoyl]-4(S)-fluoro-Pro-Pro-[3(R)-β-Pro]. This structure was developed by rational drug design with the assistance of substrate and inhibitor specificity data (Yoshimoto et al., 1994; Simmons, 2008; Simmons, 2015) and the X-ray structure of apstatin bound to *Escherichia coli* aminopeptidase P (Graham et al., 2004). ST-115 is a peptidomimetic inhibitor in which all of the peptide bonds are in the form of tertiary amide bonds to make it highly resistant to protease cleavage. The ST-115 preparation used in this study was custom synthesized by CPC Scientific, Inc., (Sunnyvale, CA), a GMP-capable company. The synthetic scheme is detailed in U.S. patent 9,212,206B1 and in related foreign patents (Simmons, 2015). The molecular weight as determined by electrospray mass spectroscopy (MS^+) is 457.6. It is a white lyophilized powder with a peptide purity of 98.1% as determined by high-performance liquid chromatography with UV detection at 220 nm. The ST-115 powder was stored at −20°C in a sealed vial placed inside a desiccated container. It is chemically stable in this form. The stability of the thiol group, both in solution and after the drying process, was discussed in *Materials and Methods*. ST-115 has a solubility in water of >50 mg/ml. It was designed for intravenous injection and for limited passive cellular uptake, as the drug target is on the outside of vascular endothelial cells. The binding affinity of ST-115 for human aminopeptidase P2 is shown in Fig. 4 as an IC_{50}. The
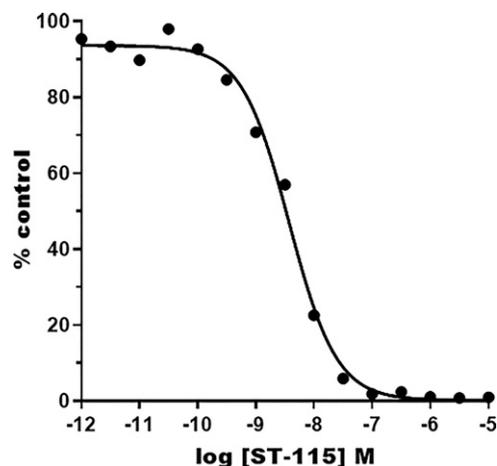
Fig. 4. Binding affinity of ST-115 for human aminopeptidase P2 expressed as an in vitro IC_{50} value. The percent decrease in purified human aminopeptidase P2 enzyme activity as a function of the log concentration of ST-115 (in molar units) was determined. The IC_{50} value was obtained by determining the concentration of ST-115 that reduced enzyme activity by 50% relative to the control activity without inhibitor.

TABLE 1
Specificity of ST-115 enzyme IC_{50} (nM)

Aminopeptidase P2	3.7
Aminopeptidase P1	660
Aminopeptidase A	>250,000
Aminopeptidase B	>100,000
Aminopeptidase N	>110,000
Aminopeptidase, cytosol alanyl	>60,000
Aminopeptidase PILS (ERAP1)	>200,000
Aminopeptidase ERAP2	>200,000
Angiotensin 1-converting enzyme	68,000
Angiotensin-converting enzyme-2	210,000
ADAM9	>200,000
Dipeptidyl-peptidase II	>100,000
Dipeptidyl-peptidase IV	>90,000
Endothelin-converting enzyme-1	>270,000
Matrix Metallopeptidase-1	270,000
Matrix Metallopeptidase-3	>200,000
Membrane dipeptidase	>60,000
Neprilysin	14,000
Neurolysin	80,000
Thimet oligopeptidase	40,000
X-Pro dipeptidase	>60,000

percent decrease of control activity was determined as a function of the log concentration (molar units) of ST-115. The curve has an R^2 of 0.9953. The IC_{50} value is 3.74 nanomolar, with a 95% CI, 2.94–4.77 nM. ST-115 is 780-fold more potent than our prototype aminopeptidase P2 inhibitor, apstatin (Maggiora et al., 1999). There was no evidence for slow-tight binding or for long residence time. Table 1 shows the specificity of ST-115 for aminopeptidase P2. None of the peptidases tested so far (20) were inhibited by ST-115 in the nanomolar range. The enzyme assays used for the specificity study are described in the Supplemental Material.

In Vivo Studies

Effect of ST-115 in the Mouse Model of Myocardial Infarction.

Infarct Size. The ability of ST-115 to reduce cardiac ischemia–reperfusion injury was tested in a mouse myocardial infarct model. Infarct size was determined after 24 hours of reperfusion and expressed as a percent of area at risk. Data were analyzed by the Prism unpaired t test as planned. The mean values were 30.1% of area at risk for saline and 12.6% of area at risk for ST-115 with a difference of −17.5 (95% CI, −29 to −6.1). ST-115 reduced the infarct size by 58% ($P = 0.007$).

A post hoc decision was made to reanalyze and visualize the data using estimation statistics and a Gardner-Altman plot (Fig. 5). The unpaired mean difference between ST-115 and saline was −17.5 (95% CI, −25.7 to −7.03). The P value of the two-sided permutation t test was 0.013. The relative risk reduction by ST-115 was predicted to be −58%, indicating a large degree of protection from myocardial infarction in mice treated with ST-115.

Effect of ST-115 in the Rat Model of Ischemic-Reperfusion Stroke.
Rats were subjected to 90 minutes of middle cerebral artery occlusion followed by 24 hours of reperfusion. ST-115 or saline was administered just before the start of reperfusion as described in *Methods* and in Fig. 3.

Skilled Horizontal Ladder Rung Walking Test. Rats underwent three baseline trials before the stroke and three trials 24 hours post reperfusion (Fig. 3). There was no statistically significant difference in baseline scores between rats that were

designated to receive either vehicle or ST-115. Fig. 6 shows the skilled walking scores of rats at 24 hours post reperfusion minus the baseline score for each rat. The unpaired mean difference between vehicle and ST-115 rats was −0.76 (95% CI, −1.49 to −0.0080). The P value of the two-sided permutation t test was 0.0636. The predicted relative risk reduction in walking deficits by ST-115 was −60%, indicating a large protective effect of ST-115 on skilled walking ability.

Brain Edema. Brain sections were analyzed for the extent of edema that occurred during ischemia and reperfusion in rats administered either saline vehicle or ST-115 just before the start of reperfusion. Fig. 7 shows the results of the estimation statistics for the percent increase in the brain section area due to edema compared with the unaffected contralateral area. The unpaired mean difference between the vehicle and ST-115 was −3.87 (95% CI, −5.95 to −1.59). The P value of the two-sided permutation t test was 0.0084. The predicted relative risk reduction that is due to ST-115 treatment of brain edema was −51%, indicating a large reduction in brain edema with ST-115.

Infarct Volume. After 24 hours, brain sections were stained with TTC to delineate the metabolically active and inactive tissues for determining infarct volume. Fig. 8 is a plot of the infarct volumes expressed as a percent of the contralateral hemisphere volume. The data were bimodal, and the overall shapes of the datapoint distributions were very similar for vehicle and ST-115 rats. Most rats (15) (65%) in both the vehicle and ST-115 groups exhibited infarct volumes less than 11% of the contralateral hemisphere, whereas the remainder of the rats (8) (35%) had infarct volumes of 18–27% of the contralateral hemisphere. This pattern is characteristic of a log-normal distribution, where there is a cluster of points with low values and a few very high-value points (Michel et al., 2020). This pattern was also observed in our preliminary studies (data not shown). There is currently no evidence for a specific methodological cause for this distribution. There are many potential mechanisms involved in ischemia–reperfusion injury (Kalogeris et al., 2016). It is possible that in our model, there is a random activation of at least two different pathways that vary in their mechanisms and lethality. The rats with large infarcts did not have corresponding large brain edema or skilled walking deficit scores (data not shown). Interestingly, ST-115 had no effect on lesion size in rats with large infarcts but did exhibit protection in rats with smaller infarcts. This observation also suggests that different damage pathways may be involved. Fig. 9 shows the extent of protection by ST-115 in those rats with smaller infarcts (i.e., less than 12% of the contralateral hemisphere volume) using estimation statistics. The unpaired mean difference between vehicle and ST-115 was −3.47 (95% CI, −6.11 to −0.531]. The P value of the two-sided permutation t test was 0.039. The predicted relative risk reduction by ST-115 in this large subgroup with smaller infarcts was −48%, indicating that ST-115 had a large protective effect against this tissue damage.

Discussion

There have been extensive efforts to develop compounds and treatments that can reduce ischemia–reperfusion injury (Downey and Cohen, 2009; Savitz et al., 2019). Most of these have failed to make it into clinical practice. Detailed analyses of these efforts have identified several reasons for this lack of success. These include choosing the wrong compounds to test,

Fig. 5. The effect of ST-115 on myocardial infarction in mice. Mice were subjected to 45 minutes of ischemia followed by reperfusion. ST-115 or vehicle (saline) was administered intravenously via the jugular vein just before the start of reperfusion. (A) After 24 hours of reperfusion, the regions not at risk were determined by phthalo blue stain. The area at risk (red plus white regions) and infarct size (white region only) were determined using TTTCstain. (B) Infarct sizes were expressed as percent of area at risk. The mean difference in infarct size between vehicle and ST-115 is shown in the Gardner-Altman estimation plot. Representative sections are shown in (C) saline and (D) ST-115.
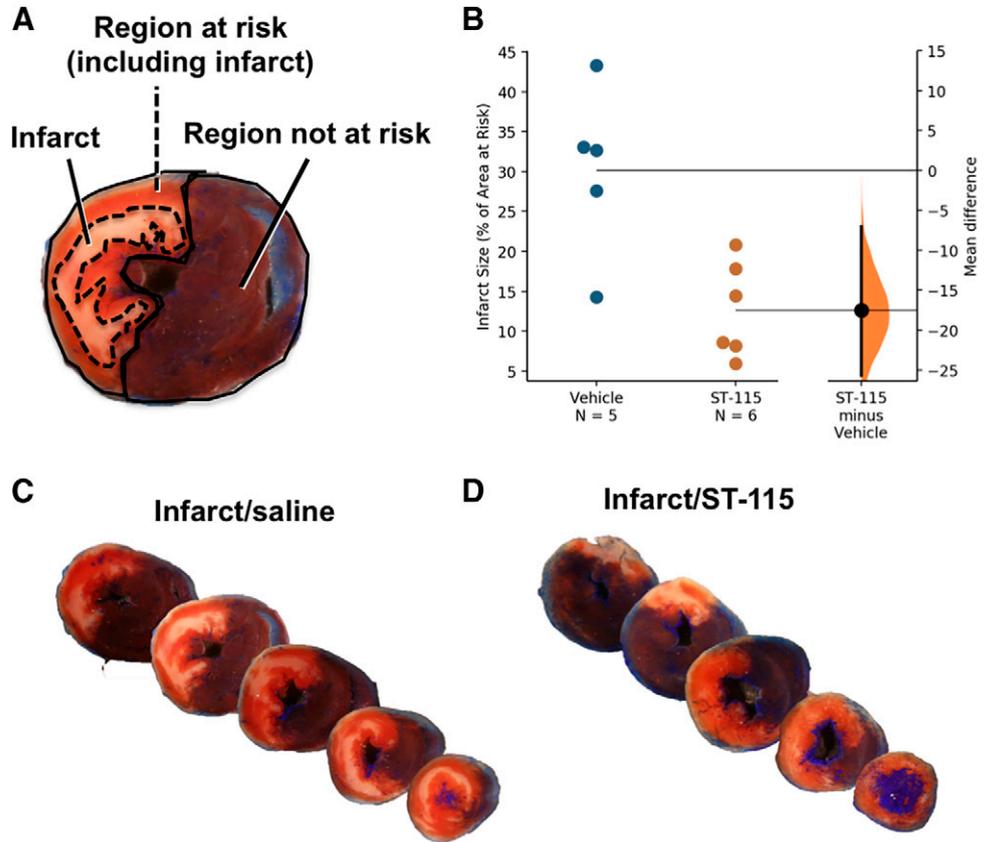
An explanation of the Gardner-Altman plot: Each datapoint represents one animal receiving either vehicle (blue) or ST-115 orange). Both groups are plotted on the left axis and arranged as a swarmplot. The horizontal lines indicate the group means. The mean difference is plotted on a floating axis on the right as a bootstrap sampling distribution. The mean difference (effect size) is depicted as a black dot. The 95% CI is indicated by the ends of the vertical error bar. The effect size and CI width are given in the text in the following way: *effect size (95% CI, lower bound–upper bound)*.

nonreplicable preclinical results, and poorly designed clinical trials (Cohen and Downey, 2017; Schãbitz and Fisher, 2006). Importantly, many drugs were tested in preclinical studies that were designed to be protective when the drug was administered before a myocardial infarction or stroke, but this is not a clinically relevant situation, as it is not possible to predict when the event will occur. Indeed, we now recognize that it is critical to demonstrate the effectiveness of cardioprotectants
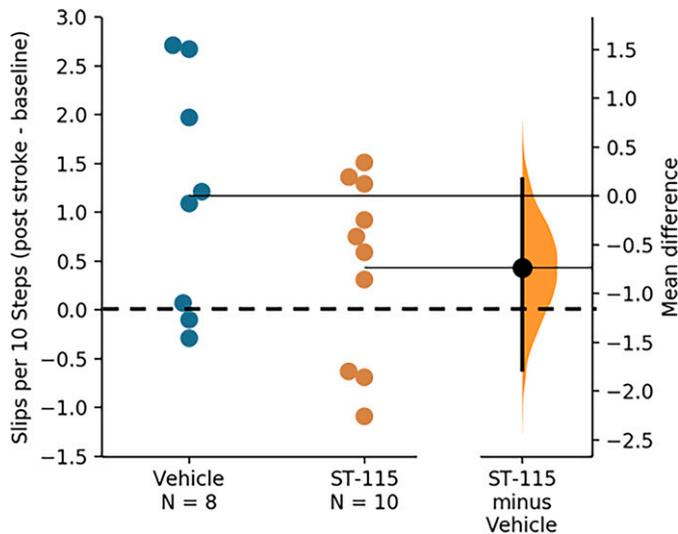
Fig. 6. The effect of ST-115 on the skilled horizontal ladder rung walking test in a rat model of ischemic-reperfusion stroke. Rats were subjected to 90 minutes of middle cerebral artery occlusion. Vehicle (saline) or ST-115 was administered intravenously just before the start of reperfusion. The rats were tested for their ability to walk across a horizontal ladder both before the stroke (baseline) and after 24 hours of reperfusion. The walking deficit data are expressed as the number of right forelimb (impaired) slips per 10 steps. The datapoints in the graph represent the post-stroke value minus the baseline value for each rat. (See the Fig. 5 legend for an explanation of the Gardner-Altman plot.)
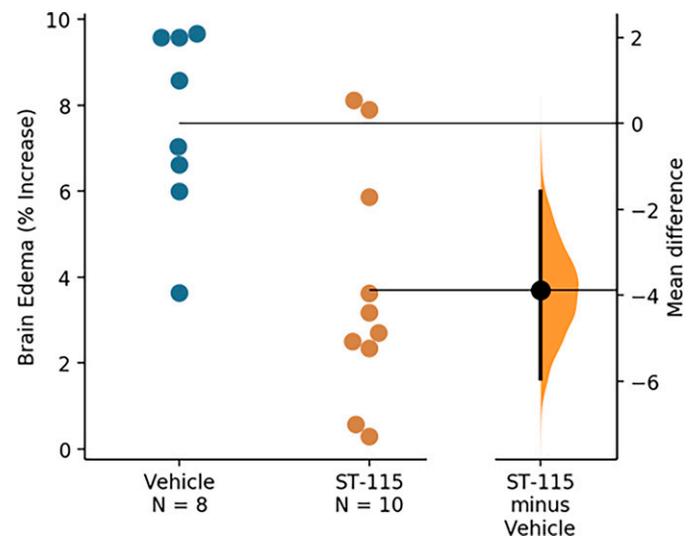
Fig. 7. The effect of ST-115 on brain edema in a rat model of ischemic-reperfusion stroke. Following a 90-minute middle cerebral artery occlusion, vehicle (saline) or ST-115 was administered intravenously just before the start of reperfusion. After 24 hours of reperfusion, the total area of brain sections of the ipsilateral hemisphere was compared with that of the unaffected contralateral hemisphere to get a measure of edema. The data are expressed as the percent increase. (See the Fig. 5 legend for an explanation of the Gardner-Altman plot.)
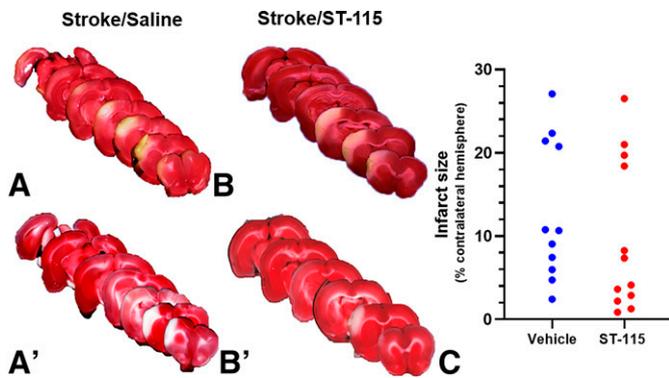
Fig. 8. The effect of ST-115 on brain infarct volume in a rat model of ischemic-reperfusion stroke. Vehicle (saline) or ST-115 was administered intravenously just before the start of reperfusion. Infarct volume was measured after 24 hours of reperfusion via TTC staining and was expressed as the percentage of the unaffected contralateral hemisphere in panel (C). Representative brain sections are shown for subgroups: (A) Saline, the four highest infarct sizes; (A') saline, the seven lowest infarct sizes; (B) ST-115, the four highest infarct sizes; (B') ST-115, the eight lowest infarct sizes.

TABLE 2.

Summary of in vivo effects of ST-115 in myocardial infarction and stroke models

Experiment	Effect Size[a]	Mean Difference	95% CI	P[b]
Myocardial infarction[c] *(mice)*				
Infarct size	↓ 58%	−17.5	−25.7 to −7.03	0.013
Stroke[d] *(rats)*				
Skilled walking deficits	↓ 60%	−0.76	−0.1.49 to −0.008	0.0636
Brain edema	↓ 51%	−3.87	−5.95 to −1.59	0.0084
Infarct size[e]	↓ 48%	−3.47	−6.11 to −0.531	0.039

[a]Relative risk reduction (%) (mean difference ÷ vehicle mean × 100).
[b]Two-sided permutation t test P value.
[c]45-minute myocardial infarction.
[d]90-minute stroke.
[e]Subset of smaller strokes

and neuroprotectants when administered at the time of reperfusion, which is a clinically relevant time point. Unfortunately, the string of failures has discouraged the scientific community and pharmaceutical companies from pursuing this line of investigation. Nevertheless, it is still recognized that there is a great need for compounds that are cardioprotective (Downey and Cohen, 2009) or brain cytoprotective (stroke) (Savitz et al., 2019). Using the correct adjunct therapy, given at reperfusion in the ischemic heart or brain, has the potential of reducing tissue injury and preserving function. The Stroke Treatments Academic Industry Roundtable has concluded that the current era of highly effective reperfusion by thrombectomy provides multiple opportunities to improve stroke therapies (Savitz et al., 2019).

ST-115 is different from many of the previously tested compounds that were designed to block only one of the many damage pathways. Instead, ST-115 likely activates multiple protective pathways via bradykinin-induced production of

endothelial nitric oxide, prostacyclin, and EETs. We found that ST-115 greatly reduced reperfusion injury in both a mouse model of acute myocardial infarction and a rat model of ischemic stroke. Importantly, this protection was evidenced when the drug was administered just prior to reperfusion in both models.

In the fully blinded mouse myocardial infarct study, the effect size was a 58% reduction in infarct size compared with vehicle. This level of protection against myocardial infarction is as strong as that seen in any previous studies. In the open-label rat stroke study, ST-115 reduced the size of three biomarkers of stroke as summarized in Table 2: 1) The deficits in the skilled horizontal ladder rung walking test were reduced by 60%, 2) brain edema was reduced by 51%, and 3) infarct size was reduced by 48% in the large subset of rats with smaller strokes. As it has been established that reperfusion injury accounts for about 50% of the total ischemia and reperfusion damage, it appears that ST-115 completely blocked reperfusion injury in these studies. The results were achieved by the intravenous administration of a small dose of ST-115 (mice: 10 µg/kg; rats: 16 µg/kg) given at 5 minutes before the start of reperfusion. During this brief time interval, ST-115 was allowed to circulate in the blood to achieve equal distribution throughout the vasculature. The drug entered the ischemic tissue when the blocked artery was opened at the start of reperfusion. ST-115 then prevented the reperfusion injury that normally occurs during the critical first ∼10 minutes of reperfusion (Husainy et al., 2012; Cohen et al., 2008). We believe that the protection took place according to the mechanism outlined in the *Introduction* and in Fig. 2, which has been corroborated by others (Baxter and Ebrahim, 2002; Veeravalli and Akula, 2004). The mechanism is very similar to the well-established mechanism that drives the cardioprotective effects of angiotensin converting ACE inhibitors. Both involve an increase in bradykinin, the release of endothelial cell mediators (Hartman 1995; Dendorfer et al., 1999), and are blocked by a bradykinin B_2 receptor antagonist. However, the ST-115 mechanism is more specific in its outcomes and also less prone to side effects. Aminopeptidase P2 (also called x-prolyl-aminopeptidase 2) is highly specific for cleaving and inactivating bradykinin because it requires that a substrate has a free N-terminal amino group, a proline residue in the second position, and a small amino acid in the third position (Yoshimoto et al., 1994; Simmons, 2013). Therefore, inhibition of this

Fig. 9. Determination of the efficacy of ST-115 on the smaller strokes from Fig. 8 that had an infarct volume less than 12% of the unaffected contralateral hemisphere. (See the Fig. 5 legend for an explanation of the Gardner-Altman plot.)

enzyme by ST-115 will primarily increase bradykinin, which is the key component of its protective function. On the other hand, ACE can cleave a very large number of different peptides. Inhibiting ACE actually increases many biologically active peptides, including substance P, which is an inflammatory peptide that is associated with the symptoms of ACE-induced angioedema (Sulpizio et al., 2004; Stone and Brown, 2017). A study by Sulpizio et al., 2005, showed that inhibition of aminopeptidase P2 by apstatin at a dose that was both cardioprotective and long lasting did not increase plasma extravasation in a rat trachea model of angioedema, whereas inhibitors of ACE and/or neprilysin did. In addition to the high specificity of aminopeptidase P2, ST-115 itself is also highly specific for inhibiting aminopeptidase P2 as shown in Table 1. It does not inhibit ACE, neprilysin, or multiple other enzymes.

In the clinic, early administration of angiotensin-converting enzyme inhibitors to patients with acute myocardial infarction can cause episodes of severe hypotension (ACE Inhibitor Myocardial Infarction Collaborative Group., 1998; Borghi and Omboni, 2020). In contrast, animal experiments have shown that inhibition of aminopeptidase P2 alone has no effect on blood pressure (Kitamura et al., 1995; Kitamura et al., 1999; Erşahin et al., 1999; Wolfrum et al., 2001) Although toxicology studies have not been done at this point, there is reason to predict that ST-115 will have minimal side effects, especially because patients will likely be exposed to the drug for only a few hours at reperfusion.

The fact that ST-115 was able to protect the brain from reperfusion injury caused by ischemic stroke requires some explanation. ST-115 is negatively charged and probably does not passively enter the brain through the blood-brain barrier. This is a problem for many compounds that are tested as a treatment of stroke (Podraza et al., 2018). But this is not an issue for ST-115, as this compound does not need to penetrate into the brain parenchyma to achieve protection. The target of ST-115 is aminopeptidase P2, which is located on the luminal side of brain vascular endothelial cells in contact with blood. After reperfusion, the concentration of ST-115 at aminopeptidase P2 is equivalent to its concentration in the blood. It is presumably the bradykinin-induced endothelial mediators of cellular protection such as prostacyclin, nitric oxide, and EETs that are able to passively enter the ischemic brain (see Fig. 2). In addition, the ability of ST-115 to reduce cerebral edema is consistent with data that show that bradykinin B_2 receptors are involved in stabilizing the blood–brain barrier and reducing inflammation during cerebral ischemia–reperfusion in diabetic rats (Sang et al., 2016).

The mechanical removal of a vascular clot from a stroke patient, referred to as thrombectomy or endovascular therapy, has become the standard of care for patients with acute ischemic stroke caused by a large vessel occlusion (Ospel et al., 2020). A combination treatment of thrombectomy and ST-115 should be especially effective, as the reperfusion is rapid and can be timed to correspond with the injection of ST-115. A combination of thrombectomy and administration of ST-115 should be able to treat both ischemic and reperfusion injury simultaneously.

ST-115 has also been tested in our laboratory in a mouse model of acute kidney injury (Simmons, 2015). After 25 minutes of bilateral renal artery occlusion and 2 days of reperfusion, blood urea nitrogen, a marker of kidney injury, was measured and found to be reduced by 56% by ST-115.

As an indication of reproducibility, these studies, along with others (Erşahin et al., 1999; Wolfrum et al., 2001; Veeravalli et al., 2003), have shown that inhibition of aminopeptidase P2 can reduce reperfusion injury in different combinations of the following: 1) two chemically different inhibitors, 2) Sprague-Dawley rats and two strains of mice, 3) in the three most sensitive tissues for ischemia–reperfusion injury (heart, brain, and kidney) (Kalogeris et al., 2016), 4) in the isolated perfused rat heart, and 5) in five different laboratories.

This report describes a discovery study. Follow-on studies of ST-115 will be carried out using the rigorous Stroke Treatments Academic Industry Roundtable criteria, which include testing in female and aged animals and in animals with comorbidities, and using assays that demonstrate long-term benefits. ST-115 may ultimately be developed for the treatment of several clinical situations that involve periods of ischemia followed by reperfusion.

References

Husainy MA, Dickenson JM, and Galiñanes M (2012) The MPTP status during early reoxygenation is critical for cardioprotection. *J Surg Res* 174:62–72.

Baxter GF and Ebrahim Z (2002) Role of bradykinin in preconditioning and protection of the ischaemic myocardium. *Br J Pharmacol* 135:843–854.

Bellis A, Sorriento D, Fiordelisi A, Izzo R, Sadoshima J, Mauro C, Cerasuolo F, Mancusi C, Barbato E, Pilato E, et al. (2020) Autocrine bradykinin release promotes ischemic preconditioning-induced cytoprotection in bovine aortic endothelial cells. *Int J Mol Sci* 21:2965.

Borghi C and Omboni S (2020) Angiotensin-converting enzyme inhibition: beyond blood pressure control–the role of zofenopril. *Adv Ther* 37:4068–4085.

Brown NJ, Gainer JV, Murphey LJ, and Vaughan DE (2000) Bradykinin stimulates tissue plasminogen activator release from human forearm vasculature through B(2) receptor-dependent, NO synthase-independent, and cyclooxygenase-independent pathway. *Circulation* 102:2190–2196.

Cheng Y and Prusoff WH (1973) Relationship between the inhibition constant (K1) and the concentration of inhibitor which causes 50 per cent inhibition (I50) of an enzymatic reaction. *Biochem Pharmacol* 22:3099–3108.

Cohen MV and Downey JM (2017) The impact of irreproducibility and competing protection from P2Y$_{12}$ antagonists on the discovery of cardioprotective interventions. *Basic Res Cardiol*

Cohen MV, Yang XM, and Downey JM (2008) Acidosis, oxygen, and interference with mitochondrial permeability transition pore formation in the early minutes of reperfusion are critical to postconditioning's success. *Basic Res Cardiol* 103:464–471.

Critz SD, Cohen MV, and Downey JM (2005) Mechanisms of acetylcholine- and bradykinin-induced preconditioning. *Vascul Pharmacol* 42:201–209.

Dendorfer A, Wolfrum S, and Dominiak P (1999) Pharmacology and cardiovascular implications of the kinin-kallikrein system. *Jpn J Pharmacol* 79:403–426.

Downey JM and Cohen MV (2009) Why do we still not have cardioprotective drugs? *Circ J* 73:1171–1177.

Erşahin C and Simmons WH (1997) Inhibition of both aminopeptidase P and angiotensin-converting enzyme prevents bradykinin degradation in the rat coronary circulation. *J Cardiovasc Pharmacol* 30:96–101.

Erşahin C, Euler DE, and Simmons WH (1999) Cardioprotective effects of the aminopeptidase P inhibitor apstatin: studies on ischemia/reperfusion injury in the isolated rat heart. *J Cardiovasc Pharmacol* 34:604–611.

Fishbein MC, Meerbaum S, Rit J, Lando U, Kanmatsuse K, Mercier JC, Corday E, and Ganz W (1981) Early phase acute myocardial infarct size quantification: validation of the triphenyl tetrazolium chloride tissue enzyme staining technique. *Am Heart J* 101:593–600.

ACE Inhibitor Myocardial Infarction Collaborative Group (1998) Indications for ACE inhibitors in the early treatment of acute myocardial infarction: systematic overview of individual data from 100,000 patients in randomized trials. *Circulation* 97:2202–2212.

Gardner MJ and Altman DG (1986) Confidence intervals rather than P values: estimation rather than hypothesis testing. *Br Med J (Clin Res Ed)* 292:746–750.

Graham SC, Maher MJ, Simmons WH, Freeman HC, and Guss JM (2004) Structure of Escherichia coli aminopeptidase P in complex with the inhibitor apstatin. *Acta Crystallogr D Biol Crystallogr* 60:1770–1779.

Gross GJ, Falck JR, Gross ER, Isbell M, Moore J, and Nithipatikom K (2005) Cytochrome *P450* and arachidonic acid metabolites: role in myocardial ischemia/reperfusion injury revisited. *Cardiovasc Res* **68**:18–25.

Hartman JC (1995) The role of bradykinin and nitric oxide in the cardioprotective action of ACE inhibitors. *Ann Thorac Surg* **60**:789–792.

Hausenloy DJ and Yellon DM (2013) Myocardial ischemia-reperfusion injury: a neglected therapeutic target. *J Clin Invest* **123**:92–100.

Ho J, Tumkaya T, Aryal S, Choi H, and Claridge-Chang A (2019) Moving beyond P values: data analysis with estimation graphics. *Nat Methods* **16**:565–566.

Kalogeris T, Baines CP, Krenz M, and Korthuis RJ (2016) Ischemia/reperfusion. *Compr Physiol* **7**:113–170.

Kitamura S, Carbini LA, Carretero OA, Simmons WH, and Scicli AG (1995) Potentiation by aminopeptidase P of blood pressure response to bradykinin. *Br J Pharmacol* **114**:6–7.

Kitamura S, Carbini LA, Simmons WH, and Scicli AG (1999) Effects of aminopeptidase P inhibition on kinin-mediated vasodepressor responses. *Am J Physiol* **276**:H1664–H1671.

Kuts R, Frank D, Gruenbaum BF, Grinshpun J, Melamed I, Knyazer B, Tarabrin O, Zvenigorodsky V, Shelef I, Zlotnik A, et al. (2019) A novel method for assessing cerebral edema, infarcted zone and blood-brain barrier breakdown in a single poststroke rodent brain. *Front Neurosci* **13**:1105.

Luther KM, Haar L, McGuinness M, Wang Y, Lynch Iv TL, Phan A, Song Y, Shen Z, Gardner G, Kuffel G, et al. (2018) Exosomal miR-21a-5p mediates cardioprotection by mesenchymal stem cells. *J Mol Cell Cardiol* **119**:125–137.

Maggiora LL, Orawski AT, and Simmons WH (1999) Apstatin analogue inhibitors of aminopeptidase P, a bradykinin-degrading enzyme. *J Med Chem* **42**:2394–2402.

Metz GA and Whishaw IQ (2002) Cortical and subcortical lesions impair skilled walking in the ladder rung walking test: a new task to evaluate fore- and hindlimb stepping, placing, and co-ordination. *J Neurosci Methods* **115**:169–179.

Michel MC, Murphy TJ, and Motulsky HJ (2020) New author guidelines for displaying data and reporting data analysis and statistical methods in experimental biology. *J Pharmacol Exp Ther* **372**:136–147.

Murry CE, Jennings RB, and Reimer KA (1986) Preconditioning with ischemia: a delay of lethal cell injury in ischemic myocardium. *Circulation* **74**:1124–1136.

Orawski AT and Simmons WH (1995) Purification and properties of membrane-bound aminopeptidase P from rat lung. *Biochemistry* **34**:11227–11236.

Ospel JM, Holodinsky JK, and Goyal M (2020) Management of acute ischemic stroke due to large-vessel occlusion: JACC Focus Seminar. *J Am Coll Cardiol* **75**:1832–1843.

Penna C, Mancardi D, Tullio F, and Pagliaro P (2008) Postconditioning and intermittent bradykinin induced cardioprotection require cyclooxygenase activation and prostacyclin release during reperfusion. *Basic Res Cardiol* **103**:368–377.

Podraza KM, Mehta Y, Husak VA, Lippmann E, O'Brien TE, Kartje GL, and Tsai SY (2018) Improved functional outcome after chronic stroke with delayed anti-Nogo-A therapy: A clinically relevant intention-to-treat analysis. *J Cereb Blood Flow Metab* **38**:1327–1338.

Prechel MM, Orawski AT, Maggiora LL, and Simmons WH (1995) Effect of a new aminopeptidase P inhibitor, apstatin, on bradykinin degradation in the rat lung. *J Pharmacol Exp Ther* **275**:1136–1142.

Ren X, Wang Y, and Jones WK (2004) TNF-alpha is required for late ischemic preconditioning but not for remote preconditioning of trauma. *J Surg Res* **121**:120–129.

Riddles PW, Blakeley RL, and Zerner B (1983) Reassessment of Ellman's reagent. *Methods Enzymol* **91**:49–60.

Sang H, Liu L, Wang L, Qiu Z, Li M, Yu L, Zhang H, Shi R, Yu S, Guo R, et al. (2016) Opposite roles of bradykinin B1 and B2 receptors during cerebral ischaemia-reperfusion injury in experimental diabetic rats. *Eur J Neurosci* **43**:53–65.

Savitz SI, Baron J-C, and Fisher M; STAIR X Consortium (2019) Stroke Treatment Academic Industry Roundtable X: brain cytoprotection therapies in the reperfusion era. *Stroke* **50**:1026–1031.

Schäbitz W-R and Fisher M (2006) Perspectives on neuroprotective stroke therapy. *Biochem Soc Trans* **34**:1271–1276.

Simmons WH (2008) inventor and assignee. Thio-containing inhibitors of aminopeptidase P and compositions thereof. U.S. patent 7,190,789 B2.

Simmons WH (2013) Aminopeptidase, in *Handbook of Proteolytic Enzymes*, 3rd ed (Rawlings ND and Salvesen GS, eds) p 2, Elsevier, New York.

Simmons WH (2015) inventor and assignee. 4-Fluoro-thio-containing Inhibitors of APP2, compositions thereof and method of use. U.S. patent 9,212,206 B1.

Simmons WH and Orawski AT (1992) Membrane-bound aminopeptidase P from bovine lung. Its purification, properties, and degradation of bradykinin. *J Biol Chem* **267**:4897–4903.

Sommer CJ (2017) Ischemic stroke: experimental models and reality. *Acta Neuropathol* **133**:245–261.

Stöckel-Maschek A, Stiebitz B, Koelsch R, and Neubert K (2003) A continuous fluorimetric assay for aminopeptidase P detailed analysis of product inhibition. *Anal Biochem* **322**:60–67.

Stone Jr C and Brown NJ (2017) Angiotensin-converting enzyme inhibitor and other drug-associated angioedema. *Immunol Allergy Clin North Am* **37**:483–495.

Sulpizio AC, Pullen MA, Edwards RM, and Brooks DP (2004) The effect of acute angiotensin-converting enzyme and neutral endopeptidase 24.11 inhibition on plasma extravasation in the rat. *J Pharmacol Exp Ther* **309**:1141–1147.

Sulpizio AC, Pullen MA, Edwards RM, Louttit JB, West R, and Brooks DP (2005) Mechanism of vasopeptidase inhibitor-induced plasma extravasation: comparison of omapatrilat and the novel neutral endopeptidase 24.11/angiotensin-converting enzyme inhibitor GW796406. *J Pharmacol Exp Ther* **315**:1306–1313.

Torchinskii YM (1974) *Sulfhydryl and Disulfide Groups of Proteins*, Consultants Bureau, New York.

Tu R, Armstrong J, Lee KSS, Hammock BD, Sapirstein A, and Koehler RC (2018) Soluble epoxide hydrolase inhibition decreases reperfusion injury after focal cerebral ischemia. *Sci Rep* **8**:5279.

Veeravalli KK, Akula A, Routhu KV, and Kota MK (2003) Infarct size limiting effect of apstatin alone and in combination with enalapril, lisinopril and ramipril in rats with experimental myocardial infarction. *Pharmacol Res* **48**:557–563.

Veeravalli KK and Akula A (2004) Involvement of nitric oxide and prostaglandin pathways in the cardioprotective actions of bradykinin in rats with experimental myocardial infarction. *Pharmacol Res* **49**:23–29.

Weston AH, Félétou M, Vanhoutte PM, Falck JR, Campbell WB, and Edwards G (2005) Bradykinin-induced, endothelium-dependent responses in porcine coronary arteries: involvement of potassium channel activation and epoxyeicosatrienoic acids. *Br J Pharmacol* **145**:775–784.

Wolfrum S, Richardt G, Dominiak P, Katus HA, and Dendorfer A (2001) Apstatin, a selective inhibitor of aminopeptidase P, reduces myocardial infarct size by a kinin-dependent pathway. *Br J Pharmacol* **134**:370–374.

Yoshimoto T, Orawski AT, and Simmons WH (1994) Substrate specificity of aminopeptidase P from *Escherichia coli*: comparison with membrane-bound forms from rat and bovine lung. *Arch Biochem Biophys* **311**:28–34.

Zhao Z-Q, Corvera JS, Halkos ME, Kerendi F, Wang N-P, Guyton RA, and Vinten-Johansen J (2003) Inhibition of myocardial injury by ischemic postconditioning during reperfusion: comparison with ischemic preconditioning. *Am J Physiol Heart Circ Physiol* **285**:H579–H588.

Address correspondence to: Dr. William H. Simmons, Loyola University Chicago Stritch School of Medicine, Department of Molecular Pharmacology and Neuroscience, Building 115, 2160 South First Avenue, Maywood, IL 60153. E-mail: wsimmon@luc.edu